Eur. Phys. J. D (2017) 71: 301
DOI: 10.1140/epjd/e2017-80356-6

THE EUROPEAN PHYSICAL JOURNAL D

Regular Article

First principles electron-correlated calculations of optical absorption in magnesium clusters*

Ravindra Shinde[1,a] and Alok Shukla[2,b]

[1] Materials Research Center, Indian Institute of Science, Bangalore, Karnataka 560012, India
[2] Department of Physics, Indian Institute of Technology Bombay, Mumbai, Maharashtra 400076, India

Received 27 May 2017 / Received in final form 29 August 2017
Published online 23 November 2017 –

Abstract. In this paper, we report large-scale configuration interaction (CI) calculations of linear optical absorption spectra of various isomers of magnesium clusters Mg_n ($n = 2$–5), corresponding to valence transitions. Geometry optimization of several low-lying isomers of each cluster was carried out using coupled-cluster singles doubles (CCSD) approach, and these geometries were subsequently employed to perform ground and excited state calculations using either the full-CI (FCI) or the multi-reference singles-doubles configuration interaction (MRSDCI) approach, within the frozen-core approximation. Our calculated photoabsorption spectrum of magnesium dimer (Mg_2) is in excellent agreement with the experiments both for peak positions, and intensities. Owing to the sufficiently inclusive electron-correlation effects, these results can serve as benchmarks against which future experiments, as well as calculations performed using other theoretical approaches, can be tested.

1 Introduction

Clusters of group II elements, such as magnesium, are particularly interesting because they have two valence electrons, quasi-filled closed shells, and in bulk they are metals. Magnesium clusters and their complexes have been a popular choice for various applications, such as hydrogen storage [1], in Grignard reagent reactions [2,3], supramolecular-based biomedicines [4], coordination polymers [5], etc., to name a few. In most of the clusters, all metal atoms reside on the surface, thereby increasing the effective surface area of interaction with the ligands. This fact can be utilized for synthesizing cluster-based supramolecules and coordinated polymers.

In the case of small magnesium clusters, the bonding between atoms is expected to be of van der Waals type. This is evident in the case of extensively studied magnesium dimer. It exhibits a large bond length of 3.92 Å and 0.034 eV/atom binding energy. However, there is a significant variation in the cohesive energy with the cluster size. For larger clusters, the bonding becomes stronger. The experimental detection of weakly bonded smaller neutral magnesium clusters is a challenging task. The identification of various clusters and their isomers can be made using the spectroscopic techniques.

Involvement of metal atoms in the clusters makes theoretical treatment a demanding task, mainly because of several nearly degenerate electronic states. In such situations, only multi-reference configuration interaction methods or coupled cluster singles doubles with perturbative triples (CCSD(T)) is known to provide best qualitative results [6]. Since in this paper, we are dealing with small-sized clusters of magnesium, treated at a large-scale multi-reference configuration interaction singles doubles level of theory, the results will be superior to other ab initio quantum chemical methods.

There have been a large number of studies of equilibrium geometries and electronic structure of small magnesium clusters [2,6–15]. The earlier studies were focused on the evolution of the electronic structure and metallicity of magnesium clusters with cluster size using various theoretical methods [7,11,12]. A majority of them involved single reference quantum chemical methods. However, very few results are available for the excited states or the optical absorption in these clusters [2,10,16]. The photoabsorption in dimer was studied experimentally in the gas phase [17] as well as in inert gas matrices [9,18]. Solov'yov et al. calculated optical absorption spectra of global minimum structures of magnesium clusters using TDDFT and compared the spectra with results of classical Mie theory [16]. However, to the best of our knowledge, no other experimental or theoretical study exists for optical absorption and excited states calculations of various low-lying isomers of magnesium clusters. The distinction of

* Supplementary material in the form of one pdf file available from the Journal web page at https://doi.org/10.1140/epjd/e2017-80356-6.

[a] e-mail: ravindra@mrc.iisc.ernet.in
[b] *Present address*: Department of Physics, Bennett University, Plot 8–11, TechZone II, Greater Noida, UP 201310, India.

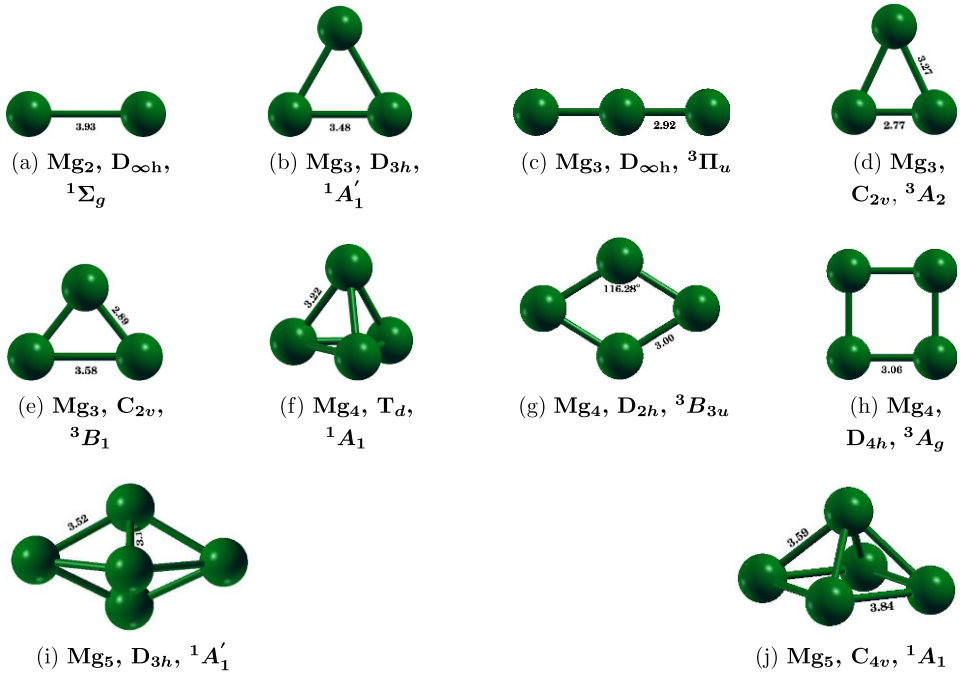

(a) Mg_2, $D_{\infty h}$, $^1\Sigma_g$ (b) Mg_3, D_{3h}, $^1A_1^{'}$ (c) Mg_3, $D_{\infty h}$, $^3\Pi_u$ (d) Mg_3, C_{2v}, $^3A_2$

(e) Mg_3, C_{2v}, $^3B_1$ (f) Mg_4, T_d, $^1A_1$ (g) Mg_4, D_{2h}, $^3B_{3u}$ (h) Mg_4, D_{4h}, ^3A_g

(i) Mg_5, D_{3h}, $^1A_1^{'}$ (j) Mg_5, C_{4v}, $^1A_1$

Fig. 1. Optimized geometries of Mg clusters considered in this work, along with the symmetries of their ground state wave functions. Geometry optimization was carried out at the CCSD level, and all lengths are in Å units.

different isomers of a cluster has to be made using experimental or theoretical techniques based upon properties which are shape and size dependent, unlike, mass spectroscopy which depends only on the mass of the cluster. We have addressed this issue by performing large-scale correlated calculations of optical absorption spectra of various isomers of magnesium clusters Mg_n ($n = 2$–5), at MRSDCI level of theory. Hence, our theoretical results can help in distinguishing between different isomers of a cluster, when coupled with the experimental measurements of their optical absorption. We also investigate the nature of optical excitations by analyzing the wavefunctions of various excited states. Furthermore, wherever possible, the results have been compared with the available literature. In earlier works, we reported similar calculations of optical absorption spectra of various isomers of small boron and aluminum clusters [19,20].

2 Theoretical and computational details

A size-consistent coupled-cluster singles doubles (CCSD) level of theory along with a 6-311+G(d) basis set was used for geometry optimization, followed by vibrational analysis [21]. This basis set is well-suited for the ground state calculations. Different spin multiplicities of the isomers were taken into account for the optimization to determine the true ground state geometry. The process of optimization was initiated by using the geometries reported by Lyalin et al. [7], based upon first principles DFT-based calculations. The final optimized geometries of the isomers are shown in Figure 1.

For computing the optical absorption spectra, both ground and excited state wave functions for these optimized geometries were calculated using multireference singles-doubles configuration interaction (MRSDCI) method implemented in the locally modified MELD package [22]. This approach consists of generating singly-and doubly-substituted configurations from a set of reference configurations, which are chosen based upon their contribution to the targeted wave functions obtained from a lower-level calculation based upon, say, single-reference singles-doubles configuration interaction (SDCI) method. Optical absorption spectra are computed at each stage of the calculation, and the targeted wave functions are analyzed to examine whether more reference configurations are needed. This procedure is repeated until the absorption spectrum of the system under consideration converges. The convergence criteria include matching of both excitation energies and dipole transition moments. Such an approach is equally efficient both for ground and excited state calculations because it takes into account the electron correlation effects for all the targeted states in an individualized manner, something which is not possible in single reference approaches. The transition dipole moment matrix elements are calculated using these ground- and excited-state wavefunctions, and are subsequently utilized to compute linear optical absorption spectrum assuming a Lorentzian line shape. The numerical approach described here has been extensively used in our earlier works dealing with the optical properties of conjugated polymers [23–27], as well as atomic clusters [19,20]. For the smallest cluster, namely, Mg dimer, it was possible to use the full CI approach, within the frozen-core approximation.

Since the computational effort involved in a CI calculation scales $\approx N^6$, where N is the total number of orbitals involved in the calculation, it can become intractable if a large basis set, leading to a large number of molecular

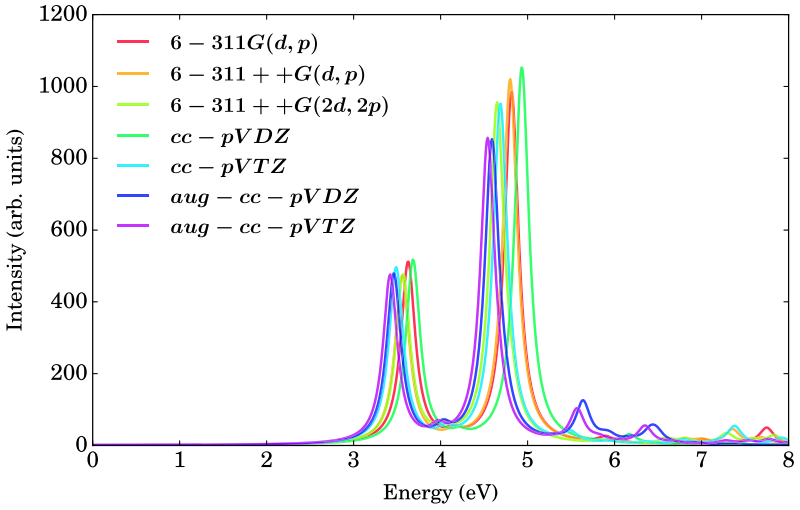

Fig. 2. Optical absorption in Mg_2 calculated using various Gaussian contracted basis sets.

Table 1. The average number of total configurations (N_{total}) involved in MRSDCI calculations, ground state (GS) energies (in Hartree) at the MRSDCI level and relative energies (in eV) of various isomers of magnesium clusters.

Cluster	Isomer	N_{ref}	N_{total}	GS energy (Ha)	Relative energy (eV)
Mg_2	(Fig. 1a) Linear	1[1]	44 796	−399.2847413	0.00
Mg_3	(Fig. 1b) Equilateral Triangular	30	239 465	−598.9270344	0.00
	(Fig. 1c) Linear	55	460 187	−598.8759291	1.39
	(Fig. 1d) Isosceles triangular-1	34	516 337	−598.8569875	1.91
	(Fig. 1e) Isosceles triangular-2	32	359 780	−598.8093768	3.20
Mg_4	(Fig. 1f) Pyramidal	32	2 962 035	−798.5781385	0.00
	(Fig. 1g) Rhombus	29	1 278 632	−798.5405148	1.02
	(Fig. 1h) Square	35	1 319 301	−798.5278160	1.37
Mg_5	(Fig. 1i) Bipyramidal	11	3 242 198	−998.2044402	0.00
	(Fig. 1j) Pyramidal	28	2 215 749	−998.1980062	0.18

[1] Frozen core full configuration interaction calculation performed for Mg dimer.

orbitals (MOs) is employed. To reduce the MO basis set size, we employed the so-called "frozen-core approximation", in which no virtual transitions are allowed from the chemical core of magnesium atoms, thereby leading to two valence electrons per atom, which were treated as active during the calculations. Furthermore, an upper limit of one hartree on the energies of the virtual orbitals to be included in the calculations was imposed, so as to control the size of the CI expansion without compromising the accuracy of the optical absorption spectrum. In the next section, we carefully examine the effects of all these approximations on our calculations.

Further computational efficiency was achieved by making full use of point-group symmetries (D_{2h}, and its subgroups), wherever applicable.

2.1 Choice of basis set

Electronic structure calculations generally depend upon the size and the quality of basis set used. To explore the basis set dependence of computed spectra, we used several basis sets [28–30] to compute the optical absorption spectrum of the magnesium dimer (Fig. 1a). For the purpose, we used basis sets named aug-cc-pVTZ, aug-cc-pVDZ, cc-pVDZ, cc-pVTZ, 6-311++G(2d,2p), 6-311++G(d,p) and 6-311G(d,p), which consist of polarization functions along with diffuse exponents [28–30]. From the calculated spectra presented in Figure 2 the following trends emerge: the spectra computed by augmented correlation consistent basis sets (aug-cc-pVDZ and aug-cc-pVTZ) are in excellent agreement with each other in the energy range up to 5 eV, while those obtained using the other basis sets (cc-pVDZ, cc-pVTZ, 6-311++G(2d,2p), 6-311++G(d,p) and 6-311G(d,p)) disagree with them substantially, particularly in the higher energy range. Peaks at 5.6 eV and 6.5 eV are seen only in the spectrum calculated using augmented basis sets. Because of the fact that augmented basis sets are considered superior for molecular calculations, we decided to perform calculations on all the clusters using the aug-cc-pVDZ basis set, to keep them tractable.

2.2 Size of the CI expansion

The electron correlation effects, both in ground state as well as excited states, were taken into account in our calculations by the inclusion of relevant configurations in the

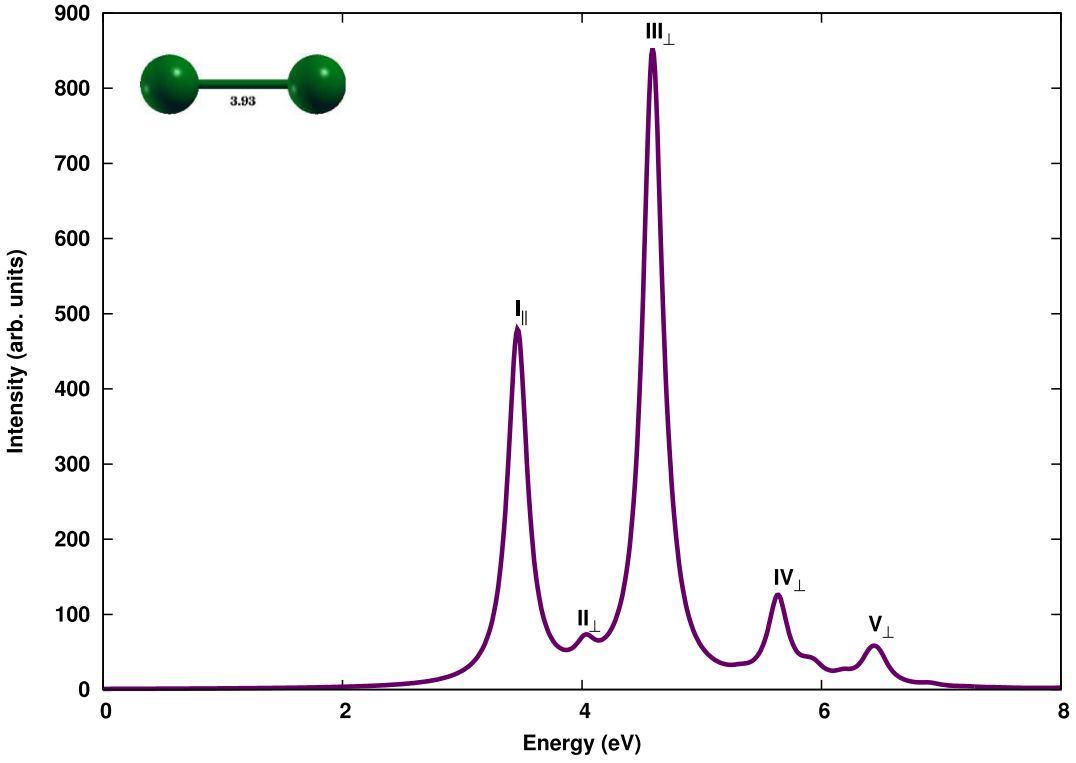

Fig. 3. The linear optical absorption spectrum of Mg_2, calculated using the MRSDCI approach. The subscript ∥ denotes the peak corresponding to the light polarization along the molecular axis, while the subscript ⊥ labels those polarized perpendiculars to it. For plotting the spectrum, a uniform linewidth of 0.1 eV was used.

reference space of MRSDCI expansion. Larger the reference configuration space, larger will be the CI expansion, which is prohibitive for bigger systems. A good chemical accuracy can be achieved by moderately sized CI expansions within the MRSDCI approach, provided the reference configurations are chosen carefully. In Table 1 we present the average number of reference states (N_{ref}) included in the MRSDCI expansion and the average number of configurations (N_{total}) for different isomers. The average is computed over different irreducible representations required in the calculation of the ground and various excited states of a given isomer. Large scale nature of these calculations is obvious from the fact that the total number of configurations in the CI expansion, N_{total}, ranges from ≈45 000 for the smallest cluster (Mg_2), to around three million for each symmetry subspace of Mg_5, implying that the electron-correlation needed for the photoabsorption calculations has been adequately included.

Before we discuss the absorption spectrum for each isomer, we present the ground state energies along with the relative energies of each isomer are given in Table 1.

3 MRSDCI photoabsorption spectra of magnesium clusters

Next we present and discuss the results of our photoabsorption calculations for each isomer. The charge densities of frontier molecular orbitals, excitation energies (with respect to the ground state), the many-body wavefunction and the oscillator strengths of the excited states corresponding to the peaks in the photoabsorption spectra of each isomer are listed in Tables S1–S10 of the Supplementary Information.

3.1 Mg_2

The simplest cluster of magnesium is Mg_2 with $D_{\infty h}$ point group symmetry. We obtained its CCSD optimized bond length to be 3.93 Å (cf. Fig. 1a), which is in excellent agreement with the experimental value 3.89 Å [17]. Using a DFT based methodology, several other theoretical values reported are in excellent agreement with our optimized bond length of magnesium dimer, i.e., Kumar and Car reported dimer bond length to be 3.88 Å [8] using density functional molecular dynamics with simulated annealing, Janecek et al. computed bond length to be 3.70 Å [31] using DFT with LDA approximation, 3.8 Å bond length was reported by Stevens and Krauss using multiconfiguration self-consistent field approach [10], 3.91 Å bond length of dimer was computed by Jellinek and Acioli using DFT with BP86 exchange-correlation functional [11], and Lyalin et al. reported 3.926 Å bond length using DFT with B3LYP exchange-correlation functional [7].

The computed photoabsorption spectra of Mg_2 (cf. Fig. 1a), as shown in Figure 3, is characterized by a couple of intense peaks in the 3–5 eV range, and by weaker absorptions, in between, and at higher energies. The first peak at 3.46 eV (cf. Tab. 2), due to the absorption of longitudinally polarized photons, is because of an

Table 2. The energies and symmetry of the excited states of major peaks in the optical absorption spectra of Mg_2 cluster (Fig. 1a).

Peak index	Energy (eV)	Symmetry
I	3.46	$^1\Sigma_u$
III	4.59	$^1\Pi_u$

excited state whose wave function is dominated by singly excited configuration $H \rightarrow L+1$, where symbols H and L denote HOMO and LUMO orbitals respectively. This peak is reported in the experimental photoabsorption at around 3.36 eV [9,17]. It is followed by a transversely polarized weaker absorption at 4.02 eV, characterized by several singly excited configurations, including $H \rightarrow L+8$. The most intense peak occurs at 4.59 eV, whose wave function is also dominated by single excitations such as $H-1 \rightarrow L$ and $H \rightarrow L+3$. The location of this peak is in excellent agreement with the experimental values of 4.59 eV reported by Lauterwald and Rademann [17,18], and 4.62 eV measured by McCaffrey and Ozin [9].

The spectrum calculated using TDLDA by Solov'yov et al. [16] is in excellent agreement with our results. In their calculations, the first peak is seen at 3.3 eV, followed by the most intense peak at 4.6 eV. The overall photoabsorption profile is also in accordance with our results. The independent particle picture is followed significantly in this weakly bonded system, thereby making TDLDA as a suitable approach.

3.2 Mg_3

We have optimized four low-lying geometries of magnesium trimer. The lowest energy structure at CCSD optimized level has equilateral triangular shape with D_{3h} symmetry (cf. Fig. 1b) and bond lengths of 3.48 Å. This agrees well with other theoretical results reporting bond lengths, 3.51 Å [31], 3.48 Å [11], and 3.475 Å [7]. The next low-lying isomer of magnesium trimer has a linear structure, with $D_{\infty h}$ symmetry (cf. Fig. 1c). The optimized bond length is found to be 2.92 Å. The remaining two low-lying isomers have isosceles triangular shape, with C_{2v} point group symmetry (cf. Figs. 1d and 1e). Not much has yet been reported on the bond lengths and electronic structure of these isomers.

Figures 4–7 present the photoabsorption spectra and Tables 3–6 list the energies and symmetries of excited states of the major peaks of these isomers.

In the equilateral triangular isomer (cf. Fig. 1b), the bulk of the oscillator strength is carried by a peak close to 3.75 eV. The linear isomer (cf. Fig. 1c) shows an altogether different absorption spectrum with a number of peaks spread out in a wide energy range, with light polarized both parallel, and perpendicular, to the axis of the trimer. On the contrary, most of the oscillator strength in the absorption spectrum of isosceles triangular isomer-I (cf. Fig. 1d) is concentrated in the range of 3–5 eV. The lower-energy part of the spectrum of isosceles triangular isomer-II (cf. Fig. 1e) is somewhat red-shifted with respect to the isosceles isomer-I, while, in the higher energy region, peaks are observed in the ultraviolet range.

The equilateral triangular isomer (cf. Fig. 1b) exhibits a weaker absorption peak at 2.6 eV, characterized by $H \rightarrow L$ and $H \rightarrow L+4$. This is followed by the most intense peak at 3.7 eV due to the light polarized both parallel and perpendicular to the plane of the isomer and with a dominant contribution from excitations $H \rightarrow L$, $H \rightarrow L+2$, and $H-1 \rightarrow L$. This is confirmed by an experimental measurement of photoabsorption of Mg trimer in the argon matrix, which exhibits a peak at 3.64 eV [9]. Semi-major peaks at around 4.7 eV and 5.8 eV obtain dominant contribution from single excitations $H \rightarrow L+7$, $H \rightarrow L+5$, and $H \rightarrow L+9$. The latter peak is due to photons polarized perpendicular to the plane of isomer.

Comparing our results for the equilateral triangular isomer with the spectrum obtained by TDDFT calculations [16], we see very good agreement on the overall profile of spectrum and excitation energies. The first peak is observed at 2.5 eV, followed by the most intense one at 3.7 eV, in the TDDFT spectrum [16]. Excitation energies and relative oscillator strengths are also in good agreement with our results.

Because the ground state of Mg_3 linear isomer (cf. Fig. 1c) is a spin triplet, its many-particle wave function predominantly consists of a configuration with two degenerate singly occupied molecular orbitals, referred to as H_1 and H_2 in rest of the discussion. The linear trimer of magnesium cluster exhibits absorption in the entire energy range explored. Very feeble peaks are observed at 0.9 eV and 2.3 eV, due to states dominated by single excitations $H_1 \rightarrow L+8$, $H_1 \rightarrow L+2$, and $H_1 \rightarrow L+4$. The wave function of the state leading to the second most intense peak at 2.9 eV is dominated by the configuration $H_1 \rightarrow L+3$. The state leading to the most intense peak at 5.4 eV derives almost equal contributions from configurations $H-2 \rightarrow L$ and $H-1 \rightarrow L+2$. The absorption due to the longitudinally polarized light contributes to the lower energy part of the spectrum, while transversely polarized light contributes to the remaining higher energy part of the spectrum.

Both isosceles triangular isomers (cf. Figs. 1d and 1e) have a spin triplet ground state; hence their excited state wave functions will consist of configurations involving electronic excitations from singly occupied degenerate H_1 and H_2 molecular orbitals, in addition to other doubly occupied orbitals. In the case of isosceles triangular isomer-I, the spectrum (cf. Fig. 6) starts with a very feeble peak at 1.13 eV, leading to a state whose wave function derives the main contribution from $H_1 \rightarrow L+1$ configuration. However, most of the absorption takes place in the energy range of 3–5 eV, with two equally intense peaks at 3.4 eV (peak V) and 4.2 eV (peak VII), while the other two peaks (VI and IX) and a shoulder (VIII) in that range, are also quite intense. Peak V is due to three closely-spaced states, the first of which is reached by photons polarized perpendicular to the plane of the triangle, while the other two are due to photons polarized in the plane of the cluster. Wave functions of all the three states derive dominant contributions from singly-excited configurations. The other most intense peak (VII) is due to two closely located states and

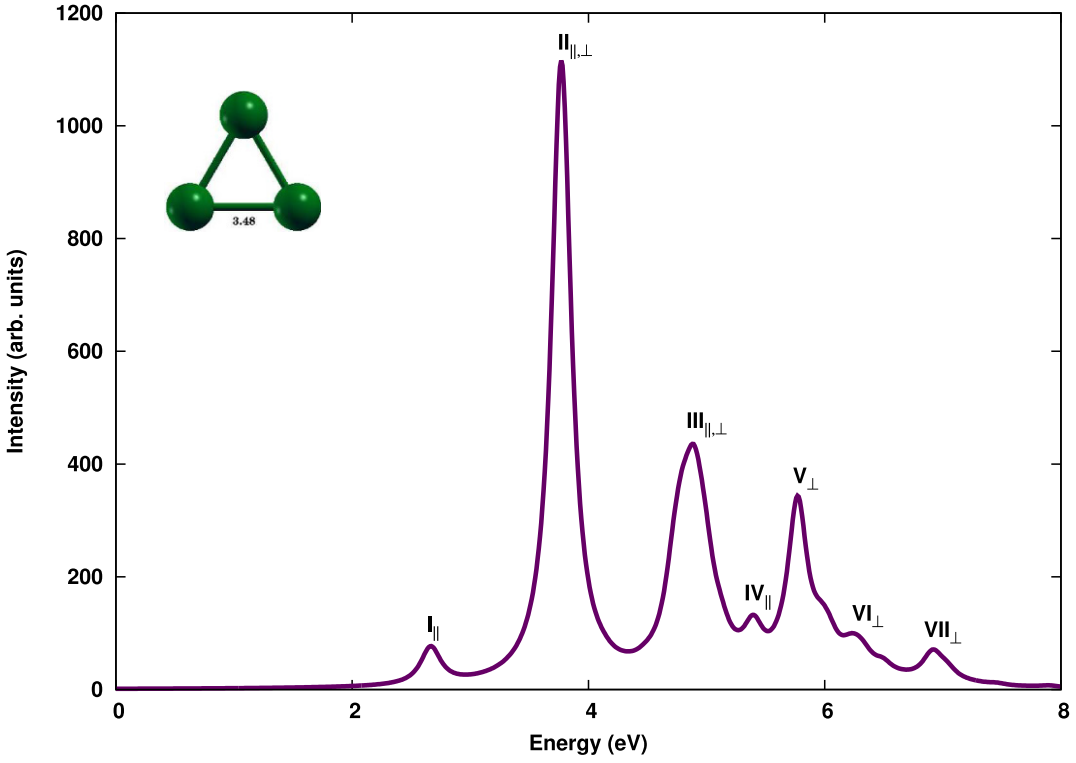

Fig. 4. The linear optical absorption spectrum of Mg_3 equilateral triangle isomer, calculated using the MRSDCI approach. The peaks corresponding to the light polarized in the molecular plane are labeled with the subscript ||, while the subscript ⊥ denotes those polarized perpendiculars to it. For plotting the spectrum, a uniform linewidth of 0.1 eV was used.

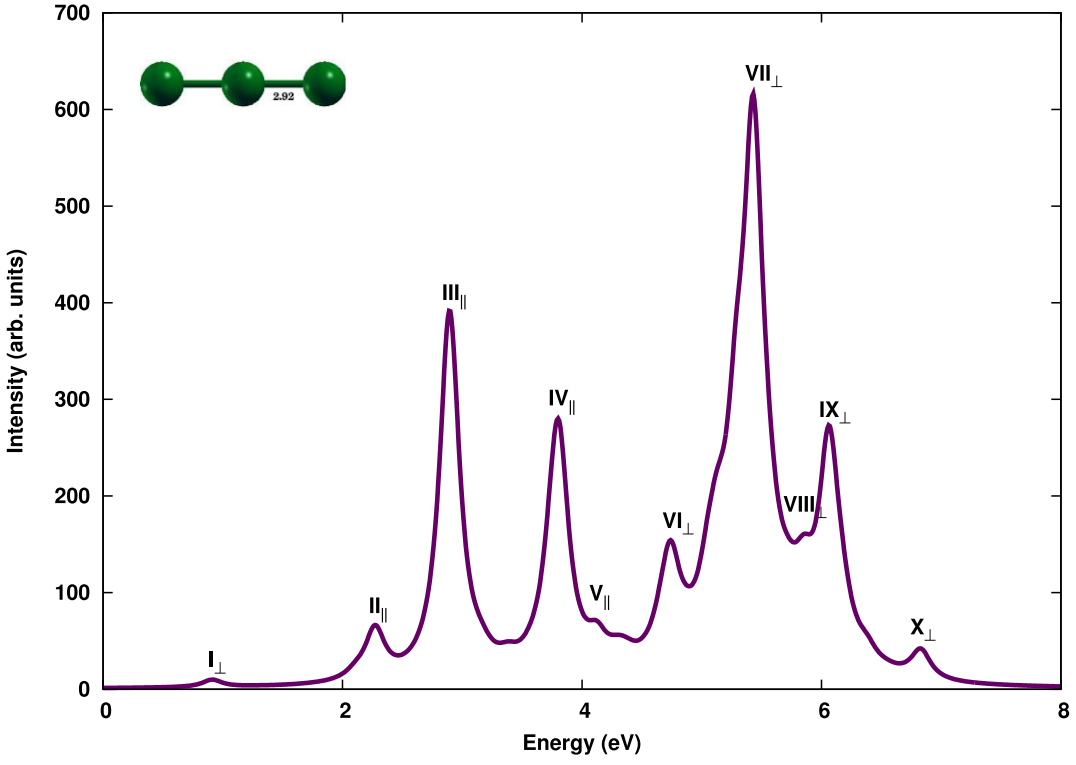

Fig. 5. The linear optical absorption spectrum of Mg_3 linear isomer, calculated using the MRSDCI approach. The peaks corresponding to the light polarized along the molecular axis are labeled with the subscript ||, while the subscript ⊥ denotes those polarized perpendiculars to it. For plotting the spectrum, a uniform linewidth of 0.1 eV was used.

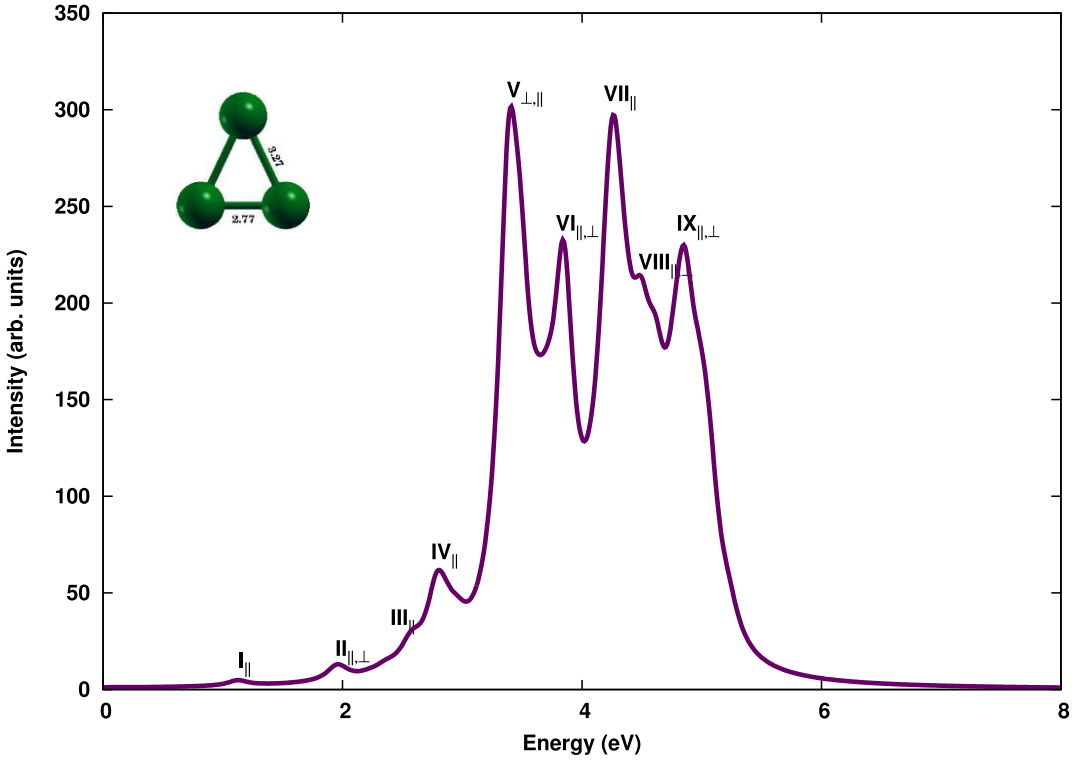

Fig. 6. The linear optical absorption spectrum of Mg_3 isosceles triangle isomer-I, calculated using the MRSDCI approach. The peaks corresponding to the light polarized in the molecular plane are labeled with the subscript $\|$, while the subscript $\perp$ denotes those polarized perpendiculars to it. For plotting the spectrum, a uniform linewidth of 0.1 eV was used.

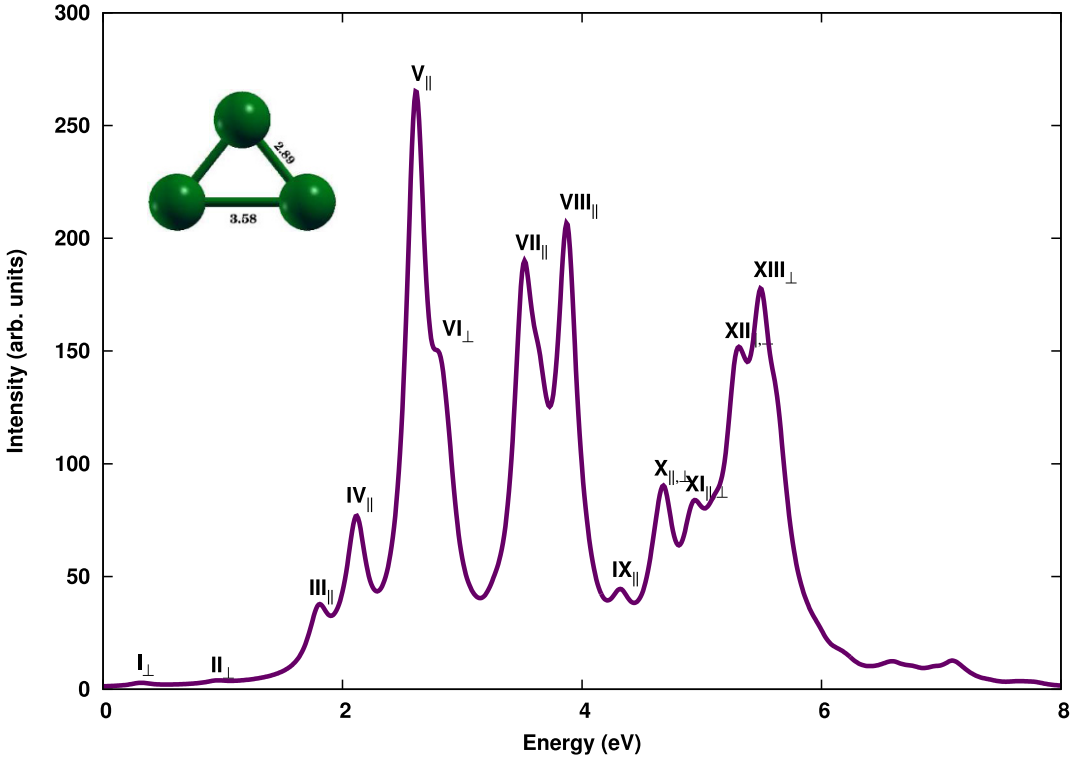

Fig. 7. The linear optical absorption spectrum of Mg_3 isosceles triangle isomer-II, calculated using the MRSDCI approach. The peaks corresponding to the light polarized in the molecular plane are labeled with the subscript $\|$, while the subscript $\perp$ denotes those polarized perpendiculars to it. For plotting the spectrum, a uniform linewidth of 0.1 eV was used.

Table 3. The energies and symmetry of the excited states of major peaks in the optical absorption spectra of Mg_3 equilateral triangle isomer (Fig. 1b).

Peak index	Energy (eV)	Symmetry
II	3.76	$^1E^{'}$
III	4.89	$^1A_2^{'}$
V	5.77	$^1A_2^{'}$

Table 4. The energies and symmetry of the excited states of major peaks in the optical absorption spectra of Mg_3 linear isomer (Fig. 1c).

Peak index	Energy (eV)	Symmetry
III	2.89	$^3\Pi_g$
IV	3.80	$^3\Pi_g$
VII	5.43	$^3\Sigma_g^-$

Table 5. The energies and symmetry of the excited states of major peaks in the optical absorption spectra of Mg_3 isosceles triangle (I) isomer (Fig. 1d).

Peak index	Energy (eV)	Symmetry
V	3.40	$^3A_1$
VI	3.83	$^3B_2$
VII	4.28	$^3A_1$

Table 6. The energies and symmetry of the excited states of major peaks in the optical absorption spectra of Mg_3 isosceles triangle (II) isomer (Fig. 1e).

Peak index	Energy (eV)	Symmetry
V	2.61	$^3A_2$
VII	3.51	$^3B_2$
VIII	3.86	$^3B_2$

displays mixed polarization characteristics. Wave functions of both these excited states, in addition to the single excitations, derive important contributions from doubly excited configurations as well.

The absorption spectrum of the isosceles triangular isomer-II (cf. Fig. 7) appears red-shifted as compared to that of the previous isomer and exhibits a set of well-separated peaks. There is just one excited state contributing to the most intense peak at 2.6 eV (peak V), which is due to the absorption of a photon polarized in the plane of the triangle. The wave function of this state mostly consists of the configuration $H_2 \rightarrow L$, with some contribution from a doubly-excited configuration $H_2 \rightarrow L; H_1 \rightarrow L + 10$. Two almost equally intense peaks of absorption due to in-plane polarized photons occur at 3.5 eV (peak VII) and 3.9 eV (peak VIII). One excited state each contributes to these peaks, and wave functions of these states are dominated by singly-excited configurations which include $H - 2 \rightarrow H_1$, $H_1 \rightarrow L + 7$, and $H_1 \rightarrow L + 17$. This isomer also exhibits a strong mixing of doubly excited configurations for excited states contributing to higher energy peaks. Significant differences in the optical absorption spectra of the two isosceles triangle shaped isomers point to a strong structure-property relationship when it comes to optical properties of these clusters.

3.3 Mg_4

The most stable isomer of Mg_4 cluster has a closed-shell electronic ground state, with the structure of a perfect tetrahedron (cf. Fig. 1f), corresponding to T_d point group symmetry, which, henceforth, we refer to as a pyramid. We computed the optimized bond length to be 3.22 Å, which agrees well with the previously reported values for this structure 3.09 Å [6], 3.33 Å [31], 3.18 Å [11], 3.31 Å [12], and 3.32 Å [13]. The rhombus isomer (cf. Fig. 1g) with D_{2h} point group symmetry, and bond length of 3.0 Å, along with the acute angle 63.5°, has $^3B_{3u}$ electronic ground state, which is 1.02 eV higher than the global minimum structure. Square isomer (cf. Fig. 1h) with D_{4h} point group symmetry, and an optimized bond length of 3.06 Å, has ^3A_g electronic ground state, which is energetically 1.37 eV higher than the most stable structure.

The absorption spectra of pyramidal, rhombus and square isomers are presented in Figures 8–10, and Tables 7–9 list the energies and symmetries of excited states of the major peaks of these isomers, respectively.

Because of the three-dimensional structure of the pyramidal isomer(cf. Fig. 1f), all three Cartesian components contribute to the transition dipole moments, thereby implying a three-dimensional polarization of the incident photons with respect to the chosen coordinate system. The onset of absorption in this isomer occurs at 2.6 eV, due to a state whose many-particle wave function is dominated by configurations $H - 1 \rightarrow L$, $H \rightarrow L$, and $H - 2 \rightarrow L$. The most intense peak in the spectrum is located at 4.54 eV due to a state whose wave function is dominated by several single excitations such as $H \rightarrow L + 2$, $H - 1 \rightarrow L + 1$, and $H - 1 \rightarrow L + 3$, etc. The TDDFT absorption spectrum of this isomer reported by Solov'yov et al. [16] is slightly red-shifted compared our calculated spectrum, however, its absorption pattern is similar to ours in that a single most intense peak at 4.2 eV is followed by several less intense peaks at higher energies.

In the case of rhombus-shaped isomer (cf. Fig. 1g), optical absorption starts with a weak peak at a rather low energy close to 1.00 eV, with the bulk of the oscillator strength distributed in the energy range 4–6 eV, consisting of several equally intense and close-lying peaks. The first weak peak at 0.98 eV corresponds to a photon polarized perpendicular to the plane of the molecule and is due to a state dominated by configuration $H_1 \rightarrow L + 1$. The most intense peak at 4.7 eV is due to a photon polarized in the plane of the isomer, and the corresponding excited state wave function is dominated by configurations $H - 1 \rightarrow L + 1$ and $H - 2 \rightarrow L$. It is preceded by a shoulder at 4.6 eV, with identical polarization properties, and an excited state wave function which derives contributions from configurations $H_2 \rightarrow L + 8$ and $H - 1 \rightarrow L$. The most intense peak corresponding to perpendicular polarization is located at 6.22 eV, with the excited state wave function dominated by doubly-excited configurations.

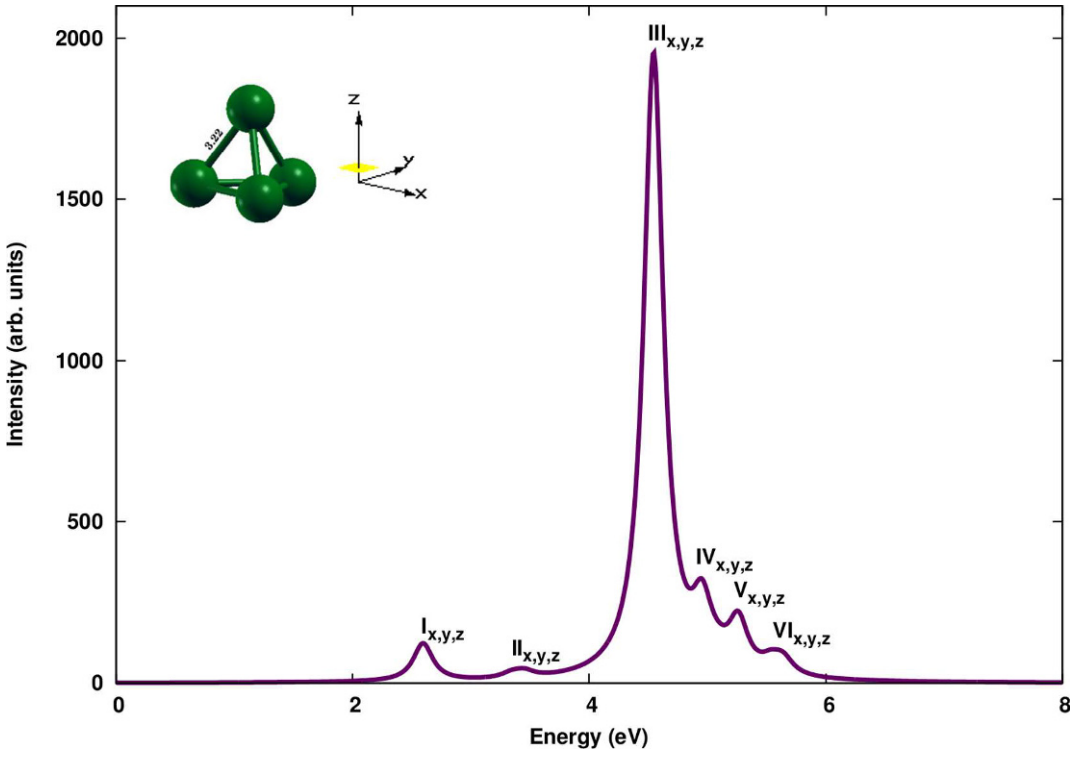

Fig. 8. The linear optical absorption spectrum of pyramidal Mg_4 isomer, calculated using the MRSDCI approach. The peaks corresponding to the light polarized along the Cartesian axes are labeled accordingly. For plotting the spectrum, a uniform linewidth of 0.1 eV was used.

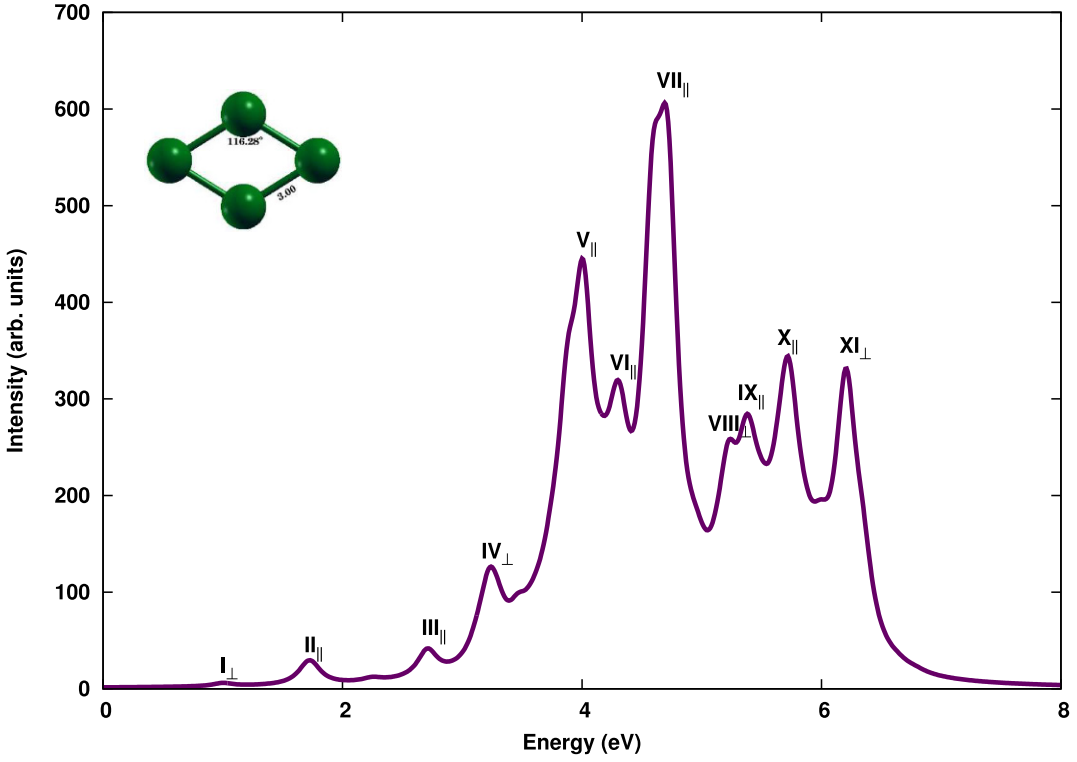

Fig. 9. The linear optical absorption spectrum of rhombus Mg_4, calculated using the MRSDCI approach. The peaks corresponding to the light polarized in the molecular plane are labeled with the subscript $\parallel$, while the subscript $\perp$ denotes those polarized perpendiculars to it. For plotting the spectrum, a uniform linewidth of 0.1 eV was used.

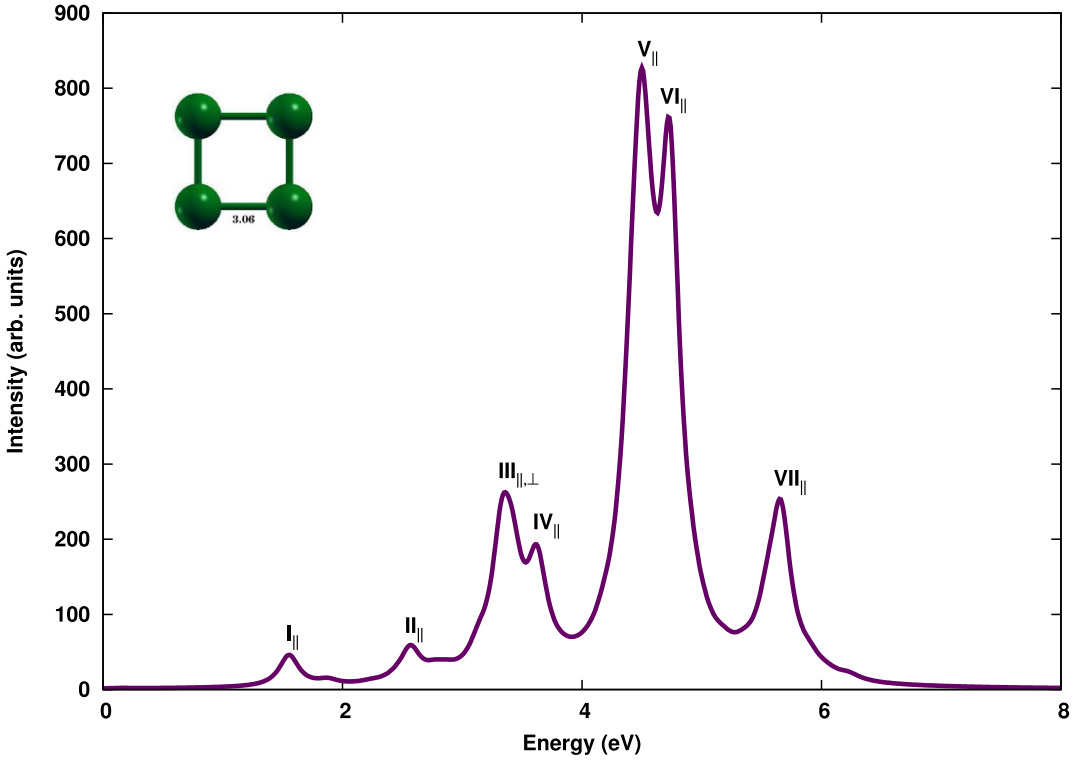

Fig. 10. The linear optical absorption spectrum of square Mg_4, calculated using the MRSDCI approach. The peaks corresponding to the light polarized in the molecular plane are labeled with the subscript $\|$, while the subscript $\perp$ denotes those polarized perpendiculars to it. For plotting the spectrum, a uniform linewidth of 0.1 eV was used.

Table 7. The energies of major peaks in the optical absorption spectra of Mg_4 pyramidal isomer (Fig. 1f).

Peak index	Energy (eV)
III	4.54

Table 8. The energies and symmetry of the excited states of major peaks in the optical absorption spectra of Mg_4 rhombus isomer (Fig. 1g).

Peak index	Energy (eV)	Symmetry
V	4.00	$^3B_{1g}$
VII	4.58	$^3B_{1g}$
	4.71	$^3B_{2g}$

Table 9. The energies and symmetry of the excited states of major peaks in the optical absorption spectra of Mg_4 square isomer (Fig. 1h).

Peak index	Energy (eV)	Symmetry
V	4.50	^3E_u
VI	4.73	^3E_u

Table 10. The energies of major peaks in the optical absorption spectra of Mg_5 bipyramidal isomer (Fig. 1i).

Peak index	Energy (eV)
V	5.37
VI	5.56

Table 11. The energies and symmetry of the excited states of major peaks in the optical absorption spectra of Mg_5 pyramidal isomer (Fig. 1j).

Peak index	Energy (eV)	Symmetry
III	3.50	^1E
IV	4.22	^1E

The inversion symmetry of the ground state of the square isomer (cf. Fig. 1h) is just opposite to that of the rhombus structure (cf. Fig. 1g), so that, as per dipole selection rule, the excited states contributing to the linear absorption spectra for the two structures also have opposite inversion symmetries. Quantitatively speaking, the absorption spectrum of the square structure is slightly blue-shifted as compared to the rhombus, and red-shifted as compared to pyramidal isomer, with the majority of absorption occurring in the energy range 3–6 eV. The onset of absorption spectrum occurs at 1.55 eV with a peak due to the light polarized in the plane of isomer, leading to a state whose wave function is a mixture predominantly of configurations $H_1 \rightarrow L+2$, $H_1 \rightarrow L+10$, and $H_1 \rightarrow L+15$. This isomer, similar to the case of the rhombus, exhibits two very closely spaced high-intensity peaks, located at 4.50 eV and 4.73 eV, both of which are due to the absorption of photons polarized in the plane of the cluster. The first of these peaks (peak V) is due to a state whose wave function is a mixture with almost equal contributions from single excitations as $H-1 \rightarrow L$,

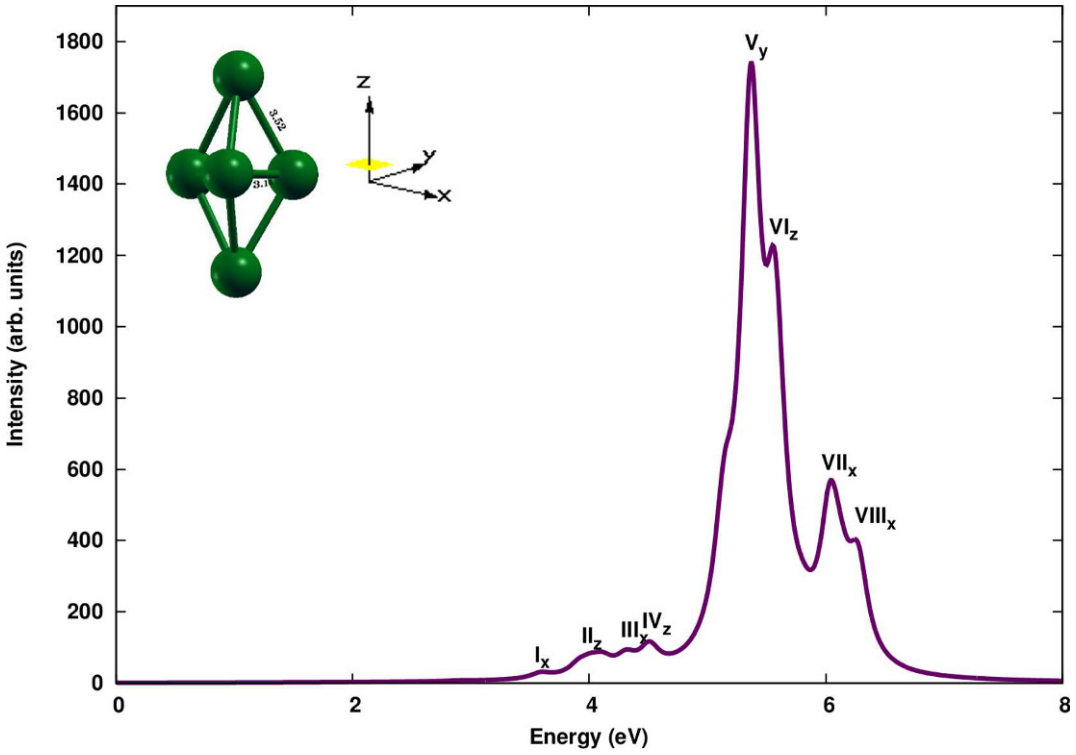

Fig. 11. The linear optical absorption spectrum of bipyramidal Mg_5 isomer, calculated using the MRSDCI approach. The peaks corresponding to the light polarized along the Cartesian axes are labeled accordingly. For plotting the spectrum, a uniform linewidth of 0.1 eV was used.

$H_1 \rightarrow L+2$, and $H_1 \rightarrow L+15$, and also a doubly-excited configuration. The excited state causing the second one (peak VI) is dominated by singly excited configurations $H_1 \rightarrow L+20$ and $H_1 \rightarrow L+24$. The last peak of the computed spectrum (peak VII) has a relatively lower intensity and is due to a state dominated by single excitations $H-2 \rightarrow L+13$ and $H_2 \rightarrow L+20$.

3.4 Mg_5

We optimized geometries of two isomers of Mg_5: (a) bipyramid with the D_{3h} symmetry (cf. Fig. 1i) and (b) a pyramidal structure with the C_{4v} point group symmetry (cf. Fig. 1j). The lowest lying bipyramidal isomer has $^1A_1^{'}$ electronic ground state and is just 0.18 eV lower in energy as compared to the pyramid structure. Our optimized geometry for the bipyramid has bond lengths of 3.15 Å and 3.52 Å, as against 3.00 Å, 3.33 Å reported by Jellinek and Acioli [11], and 3.09 Å, 3.44 Å reported by Lyalin et al. [7].

The bipyramidal isomer of Mg_5 cluster (cf. Fig. 1i) exhibits an absorption spectrum very different from other isomers, as displayed in Figure 11. The optical absorption spectrum of bipyramid Mg_5 has no absorption until 3.5 eV, while most of the absorption takes place in a narrow energy range 5.3–6.3 eV. The absorption spectrum begins at 3.6 eV through a photon polarized in the basal plane of the bipyramid, with a very feeble peak corresponding to a state whose wave function derives the main contribution from $H-1 \rightarrow L+4$ configuration. This is followed by several such smaller peaks. The most intense peak at 5.4 eV (cf. Tab. 10) has a dominant contribution from $H \rightarrow L+1$ along with other singly excited configurations, with absorption polarized again along the basal plane of the pyramid. A shoulder at 5.6 eV, however, corresponds to the absorption of light with polarization along the z-direction, which is perpendicular to the basal plane. This feature is caused by an excited state whose wave function is mainly a linear combination of several singly-excited configurations. The TDDFT spectrum computed by Solov'yov et al. [16] shows optical activity in the energy range of 2–4 eV, which is not observed in our calculated spectrum. However, a quasi-continuous spectrum is seen at higher energies in both calculations. The results of TDDFT are limited by various factors such as the functional adiabatic approximation, underestimation of charge-transfer, Rydberg and triplet excitations [32]. Hence a complete agreement cannot be expected between this linear-response TDDFT and large-scale multi-reference CI calculations which overcome limitations.

The optical absorption spectrum of pyramid shaped isomer (cf. Fig. 1j), to the best of our knowledge, has not been computed, so far, by any other author. The entire absorption spectrum (cf. Fig. 12) the pyramid shaped isomer is highly red-shifted as compared to the bipyramid isomer. The optical absorption of this isomer exhibits a few feeble peaks in the low energy range, with the onset of spectrum occurring at 2.24 eV through photons polarized in the basal plane of the pyramid, as well as perpendicular to it. The wave functions of the two excited states contributing to this peak are dominated by configurations

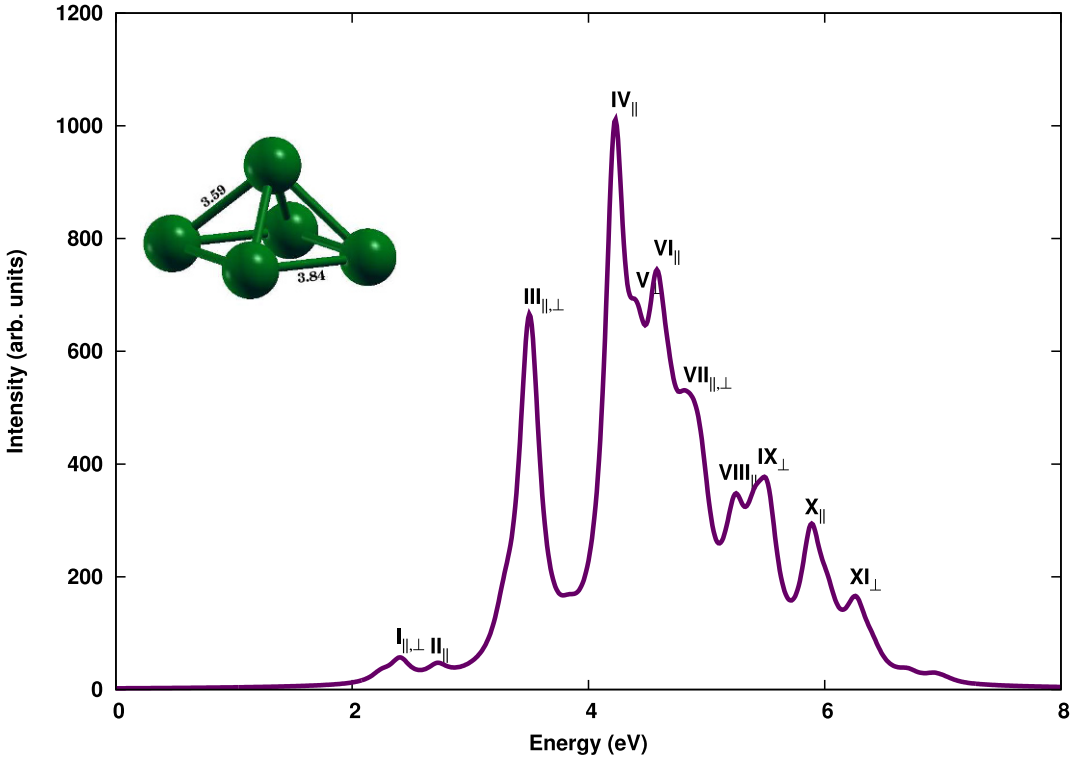

Fig. 12. The linear optical absorption spectrum of pyramidal Mg_5, calculated using the MRSDCI approach. The peaks corresponding to the light polarized along the base of the pyramid are labeled with the subscript $\parallel$, while the subscript $\perp$ denotes those polarized perpendiculars to it. For plotting the spectrum, a uniform linewidth of 0.1 eV was used.

$H-1 \rightarrow L$ and $H \rightarrow L+2$. The second most intense peak close to 3.5 eV (cf. Tab. 11) is well separated from the most intense one located at 4.2 eV. The former has mixed polarization characteristics, with two states dominated by configurations $H-1 \rightarrow L+3$ and $H-2 \rightarrow L$, besides several other single excitations. The most intense peak is due to light polarized perpendicular to the basal plane of the pyramid, and wave function of the excited state involved is dominated by configurations $H-2 \rightarrow L+1$ and $H-2 \rightarrow L+3$. The last absorption peak in the probed energy range is located at 6.27 eV, caused by a photon polarized perpendicular to the base of the pyramid, and is due to an excited state deriving the main contribution from a doubly-excited configuration, along with several single excitations. Pyramid shaped isomer exhibits prominent optical absorption in the higher energy range, with almost regularly spaced peaks of declining intensities, in contrast to single major peak observed in the spectrum of bipyramidal isomer. These differences can help in experimental identification of geometries of various isomers, through optical absorption spectroscopy.

4 Conclusions and outlook

In this work, large-scale first-principles electron correlated calculations of photoabsorption spectra of several low-lying isomers of magnesium clusters Mg_n ($n=2$–5), were presented. For the case of magnesium dimer, we employed one of the best possible electronic structure methods, namely FCI method, within the frozen-core approximation, to compute its electronic states. Calculations for the remaining clusters were performed using MRSDCI approach, which takes excellent account of the electron-correlation effects both for ground and excited states. We have also analyzed the nature of the many-particle wave functions of the excited states visible in the absorption spectra. Distinct signature spectra are exhibited by isomers of a given cluster, suggesting a strong structure-property relationship. This behavior can be utilized in the experiments to distinguish between different isomers of a cluster, using optical absorption spectroscopy. Given the fact electron-correlation effects were included in our calculations in a sophisticated manner by means of large-scale CI expansions, we believe that our results can be used as theoretical benchmarks of absorption spectra of Mg clusters, against which both the experimental and other theoretical results can be compared. We hope that our work will lead to experimental measurements of the optical absorption spectra of magnesium clusters of various shapes and sizes.

R.S. acknowledges the Council of Scientific and Industrial Research (CSIR) and Science and Engineering Research Board (SERB) India, for research fellowships (09/087/(0600)2010-EMR-I), (PDF/2015/000466). Authors kindly acknowledge computational resources provided by National Param Yuva Supercomputing Facility, C-DAC, Pune.

Author contribution statement

A.S. conceptualized the problem and the calculation procedure, R.S. performed the calculations. Both authors analyzed the results and wrote the manuscript.

References

1. R.W.P. Wagemans, J.H. van Lenthe, P.E. de Jongh, A.J. van Dillen, K.P. de Jong, J. Am. Chem. Soc. **127**, 16675 (2005)
2. S.N. Belyaev, S.V. Panteleev, S.K. Ignatov, A.G. Razuvaev, Comput. Theor. Chem. **1079**, 34 (2016)
3. A.V. Tulub, V.V. Porsev, in *Self-organization of molecular systems: from molecules and clusters to nanotubes and proteins*, edited by N. Russo, V.Y. Antonchenko, E.S. Kryachko (Springer Netherlands, Dordrecht, 2009), pp. 385–397
4. C. Zhang, R.S. Patil, T. Li, C.L. Barnes, J.L. Atwood, Chem. Commun. **53**, 4312 (2017)
5. S.-L. Cai, Z.-H. He, W.-H. Wu, F.-X. Liu, X.-L. Huang, S.-R. Zheng, J. Fan, W.-G. Zhang, CrystEngComm **19**, 3003 (2017)
6. A. Kohn, F. Weigend, R. Ahlrichs, Phys. Chem. Chem. Phys. **3**, 711 (2001)
7. A. Lyalin, I.A. Solov'yov, A.V. Solov'yov, W. Greiner, Phys. Rev. A **67**, 063203 (2003)
8. V. Kumar, R. Car, Phys. Rev. B **44**, 8243 (1991)
9. J.G. McCaffrey, G.A. Ozin, J. Chem. Phys. **88**, 2962 (1988)
10. W.J. Stevens, M.J. Krauss, Chem. Phys. **67**, 1977 (1977)
11. J. Jellinek, P.H. Acioli, J. Phys. Chem. A **106**, 10919 (2002)
12. J. Akola, K. Rytkönen, M. Manninen, Eur. Phys. J. D **16**, 21 (2001)
13. I.G. Kaplan, S. Roszak, J. Leszczynski, J. Chem. Phys. **113**, 6245 (2000)
14. X. Xia, X. Kuang, C. Lu, Y. Jin, X. Xing, G. Merino, A.J. Hermann, Phys. Chem. A **120**, 7947 (2016)
15. K. Duanmu, J. Friedrich, D.G. Truhlar, J. Phys. Chem. C **120**, 26110 (2016)
16. I.A. Solov'yov, A.V. Solov'yov, W. Greiner, J. Phys. B **37**, L137 (2004)
17. W.J. Balfour, A.E. Douglas, Can. J. Phys. **48**, 901 (1970)
18. H. Lauterwald, K. Rademann, Ber. Bunsenges. Phys. Chem. **96**, 1273 (1992)
19. R. Shinde, A. Shukla, Nano LIFE **2**, 1240004 (2012)
20. R. Shinde, A. Shukla, Phys. Chem. Chem. Phys. **16**, 20714 (2014)
21. M.J. Frisch et al., *Gaussian 09 Revision A.02* (Gaussian Inc., Wallingford, CT, 2009)
22. L.E. McMurchie, S.T. Elbert, S.R. Langhoff, E.R. Davidson, MELD package from Indiana University. It has been modified by us to handle bigger systems, 1990
23. A. Shukla, Phys. Rev. B **65**, 125204 (2002)
24. P. Sony, A. Shukla, Phys. Rev. B **71**, 165204 (2005)
25. P. Sony, A. Shukla, Phys. Rev. B **75**, 155208 (2007)
26. H. Chakraborty, A. Shukla, J. Phys. Chem. A **117**, 14220 (2013)
27. H. Chakraborty, A. Shukla, J. Chem. Phys. **141**, 164301 (2014)
28. K.L. Schuchardt, B.T. Didier, T. Elsethagen, L. Sun, V. Gurumoorthi, J. Chase, J. Li, T.L. Windus, J. Chem. Inf. Model. **47**, 1045 (2007)
29. D. Feller, J. Comput. Chem. **17**, 1571 (1996)
30. B.P. Prascher, D.E. Woon, K.A. Peterson, T.H. Dunning, A.K. Wilson, Theor. Chem. Acc. **128**, 69 (2010)
31. S. Janecek, E. Krotscheck, M. Liebrecht, R. Wahl, Eur. Phys. J. D **63**, 377 (2011)
32. A. Prlj, B.F.E. Curchod, A. Fabrizio, L. Floryan, C. Corminboeuf, J. Phys. Chem. Lett. **6**, 13 (2015)